

Nanoscale

Accepted Manuscript



This is an *Accepted Manuscript*, which has been through the Royal Society of Chemistry peer review process and has been accepted for publication.

Accepted Manuscripts are published online shortly after acceptance, before technical editing, formatting and proof reading. Using this free service, authors can make their results available to the community, in citable form, before we publish the edited article. We will replace this *Accepted Manuscript* with the edited and formatted *Advance Article* as soon as it is available.

You can find more information about *Accepted Manuscripts* in the [Information for Authors](#).

Please note that technical editing may introduce minor changes to the text and/or graphics, which may alter content. The journal's standard [Terms & Conditions](#) and the [Ethical guidelines](#) still apply. In no event shall the Royal Society of Chemistry be held responsible for any errors or omissions in this *Accepted Manuscript* or any consequences arising from the use of any information it contains.

Rapid-releasing of HI-6 via Brain-targeted Mesoporous Silica Nanoparticles for Nerve Agent Detoxification

Jun Yang¹, Lixue Fan¹, Feijian Wang¹, Yuan Luo¹, Xin Sui¹, Wanhua Li¹, Xiaohong Zhang² and Yongan Wang^{1}*

¹State Key Laboratory of Toxicology and Medical Countermeasures, Institutes of Pharmacology and Toxicology, Academy of Military Medical Sciences, Beijing, 100850, China

²Institute of Functional Nano & Soft Materials, Soochow University, Soochow, 215123, China

Abstract

The toxic nerve agent (NA) soman is the most toxic artificially synthesized compound that can rapidly penetrate into the brain and irreversibly inhibit acetylcholinesterase (AChE) activity, leading to immediate death. However, there are currently few brain-targeted nanodrugs that can treat acute chemical brain poisoning owing to limited drug-releasing speed. The present study investigated the effectiveness of a nanodrug against NA toxicity that has high blood–brain barrier penetration and is capable of rapid drug release. Transferrin-modified mesoporous silica nanoparticles (TF-MSNs) were conjugated with the known AChE reactivator HI-6. This nanodrug rapidly penetrated the blood-brain barrier in zebrafish and mice and restored cerebral AChE

activity via the released HI-6, preventing the brain damage caused by soman poisoning and increasing the survival rate in mice. Furthermore, there was no toxicity associated with the MSNs in mice or rats. These results demonstrate that TF-MSNs loaded with HI-6 represent the most effective antidote against NA poisoning by soman reported to date, and suggest that MSNs are a safe alternative to conventional drugs and an optimal nanocarrier for treating brain poisoning, which requires acute pulse cerebral administration.

1 Introduction

Nerve agents (NAs) such as sarin, soman, tuban, and VX are maintained as chemical weapons by many countries.^{1,2} In 1995, the Tokyo subway system sustained a terrorist attack in which sarin gas was used;³ in 2013, the use of NAs during the civil war in Syria led to mass casualties.⁴ Exposure to NAs can irreversibly inhibit acetylcholinesterase (AChE) in the brain⁵ and cause seizures, respiratory arrest, or even immediate death.⁶ Current medical treatment for NA poisoning has been impeded by the fact that these toxicants can rapidly penetrate the central nervous system, whereas all of the current therapeutic drugs, called reactivators, are only able to reactivate the AChE but are unable to be transported into the brain,⁷ as the molecular group of quaternary amine and oxime of the reactivators⁸ are essential for AChE reactivation but hamper blood brain barrier (BBB) penetration.^{9, 10} This inherent drawback makes it difficult to develop a novel antidote that can be used for detoxification following NA brain poisoning.^{8, 11} Therefore, the use of brain-targeted nanodrugs (BTN) to transport

existing reactivators into the brain is currently the most plausible strategy for overcoming NA poisoning.¹² The most existing studies of BTNs to date have focused on cancer^{13, 14} or Alzheimer's¹⁵ and other neurological diseases,¹⁶ for which the treatment necessitates drug concentrations to be maintained in the lesion area over a long duration. To this end, BTNs, in which drugs are loaded and sealed within a polymer or other nano-size biomaterial coating,¹⁷ exhibit slow, sustained drug release in the lesion area.¹⁸ However, conventional BTNs are not suitable for application in acute NA poisoning treatment, nor in conditions such as epilepsy, acute cerebral infarction, and acute cerebral hemorrhage, as the slow release from BTNs provided insufficient reactivator to counter the rapid brain damage caused by NA. As such, new BTNs that can rapidly deliver adequate amounts of reactivator to the brain and efficiently release the drugs are urgently needed owing to the ever-present threat of terrorists and the over-spread of chemical weapons.

The consideration of BTNs as a cure for NA poisoning has previously not been suitably addressed by current research. On the one hand, some researchers have not realized the urgency associated with a lack of antidote against NA and have paid little attention to this field during peacetime. On the other hand, it is difficult to integrate the two key functions of BTNs (high loading capacity and rapid releasing speed) in a single nanoparticle owing to the bottlenecks of the constitution and structure of nanosystems.¹⁹ Conventional BTNs without a layer coating structure have high loading capacity but slow release speed because of the lack of direct release channels. Conversely, another kind of BTNs in which the hydrophilic reactivator is adsorbed on

the outside of human serum albumin nanoparticles (NPs)^{12, 20} allow the drugs to be quickly transported into the environment; however, the quantity of reactivator transported to the brain is insufficient for effective NA poisoning treatment owing to the insufficient storage space (low loading capacity) of these BTN. Therefore, for realizing an effective therapeutic effect for NA poisoning, the structure of BTNs must have a directly release channel and enough storage space to ensure both rapid release and high loading.

Base on the stated requirements, we believe that NPs with a sponge-like mesoporous structure²¹ might realize these functions by meeting the delivery requirements regarding releasing time and loading quantity. Sufficient quantities of drugs could be stored in the numerous inner pores and released via the channel quickly and directly without the barrier of an outside coating polymer layer. Mesoporous silica nanoparticles (MSNs) are a classic sponge-like nanomaterial²¹ that exhibit good biocompatibility.²² Previous studies have ignored the characteristic of rapid releasing speed of this nanomaterial and even avoided it during applications in cancer therapy.²²⁻²⁴ However, for transporting an antidote against NA, MSN might be the appropriate candidate owing to its regular mesoporous structure for storage and release, favorable surface-coatability, and high biosafety. Furthermore, MSN has been shown to rapidly adsorb and effectively destruct a NA in previous reports²⁵⁻²⁷, and therefore is usually applied as a decontaminating agent. The further application of MSN to drug delivery across the BBB would open up a new method for curing acute cerebral disease. For example, in the present study we investigated the potential for using MSNs to

antagonize brain NA poisoning by soman, which is one of most toxic compounds without any known antidotes.

Here, we developed a detoxification system (DS) consisting of MSNs modified with a brain-targeting protein layer²⁸ and loaded with the reactivator, HI-6,^{29, 30} which we predicted would effectively reactivate soman-inhibited AChE in the brain (Fig 1A). This represents the first report of the utilization of this classic nanomaterial for rapid cerebral drug delivery, in particular for NA detoxification in the brain. Furthermore, the *in vivo* efficacy of the system against actual NA soman poisoning was tested in mice that were deficient in other related reports^{12, 20, 31}. The safety of MSNs especially in the brain was also tested in both mice and rats.

2 Experimental

2.1 MSN preparation. MSNs were prepared using the silane-controlled hydrolysis method.²² Fluorescein isothiocyanate (FITC) (3 mg) and aminopropyltriethoxysilane (12 μ l) were dissolved in ethanol (3 ml) under an N₂ atmosphere for 5 h. The reaction product and tetraethylorthosilicate (500 μ l) were injected into distilled water (120 ml) containing aqueous sodium hydroxide (2 M; 857 μ l) and cetyltrimethylammonium bromide (CTAB; 0.25 g) and stirred vigorously at 80°C for 4 h. After aging for 2 h, MSNs with a diameter < 150 nm were obtained and centrifuged in ethanol three times to wash out residual CTAB and NaOH. The particles were then refluxed in a mixture of hydrochloric acid (12.1 M; 18 ml) and methanol (100 ml) for 24 h to remove CTAB from the pores.

2.2 Preparation of transferrin-modified MSNs (TF-MSNs). MSNs (80 mg) were sonicated and dispersed in toluene (10 ml) before adding 3-glycidoxypropyltrimethoxy-silane (200 μ l); the suspension was then stirred under N_2 for 5 h at 60°C. The particles were collected by centrifugation and re-suspended in 4-(2-hydroxyethyl)-1-piperazineethanesulfonic acid (HEPES) buffer (0.05 M). TF (2 ml) was added to the suspension, which was stirred for an additional 30 min at room temperature. The product was separated by centrifugation and stored at -20°C ; the supernatant was also collected for subsequent measurements.

2.3 TF load. The unreacted TF was dissolved in the supernatant collected in the former step. After being diluted several times, the dosage of protein ($m_{TFunreact}$) was assessed using a bicinchoninic acid (BCA) protein assay kit. The density of MSN (β) was measured by the Brunner-Emmett-Teller method (BET). MSN was modeled as a model of sphere with diameter of 100 nm. The number of TFs reacted on the surface of each MSN was calculated using the equation:

$$N = 4\pi r^3 \beta * NA * (m_{TFinput} - m_{TFunreact}) / 3m_{MSNinput}M_{TF}$$

2.4 Drug loading of TF-MSNs. HI-6 was directly added to the TF-MSN suspension and stirred for 30 min at room temperature. The final concentrations used were 3 and 2.2 mg ml^{-1} for MSNs and HI-6, respectively.

2.5 Drug loading and encapsulation ratio. HI-6 (3.3 mg, 6.6 mg, or 13.2 mg) was directly added to the MSN/TF-MSN suspension (3 mg ml^{-1} , 3 ml) and stirred for 30 min at room temperature. The final concentrations of HI-6 were 1.1, 2.2, and 4.4 mg ml^{-1} , respectively. The NPs were collected by centrifugation and the supernatant was removed. The collected samples were added to 5 ml saline and then stirred for 1 h. The samples were centrifuged again and the new supernatant was collected and measured by UV absorbance. The concentration of the HI-6 loaded in the MSNs was determined by a characteristic wavelength of 300 nm.

2.6 Preparation of TF-modified poly lactic-co-glycolic acid (PLGA) NPs (TPNPs).

NPs were formed from HI-6 by the water-in-oil micro-emulsion method.³² Briefly, 100 μl stock HI-6 aqueous solution (50 mg ml^{-1}) was injected into 5 ml acetone with vigorous stirring at room temperature. NPs were centrifuged three times to wash out the water. The HI-6 NP suspension was added to 2 ml PLGA/acetone (1 mg ml^{-1}) and stirred, and the mixture was added drop-wise to 1% (v/v) Tween 20 solution with vigorous stirring until the emulsion became transparent. The product was centrifuged three times to wash out the Tween 20 and then dispersed in Ringer-HEPES buffer (pH 7.4) at a concentration of 1 mg ml^{-1} before 0.5 ml TF solution, 50 mg 1-(3-dimethylaminopropyl)-3-ethylcarbodiimide hydrochloride, and 50 mg N-hydroxysuccinimide were added to the system. After stirring for 12 h at 40°C , NPs were collected, washed, centrifuged three times, and characterized.

2.7 Drug release. TF-MSNs (2 ml) loaded with HI-6 suspension (2.2 mg ml^{-1}) were sealed in dialysis tubes (molecular weight cut-off: 4,000 Da), which were immersed in 198 ml saline at room temperature with gentle stirring. A 2-ml volume of sample was collected at predetermined time intervals and replaced with 2 ml fresh saline. The concentration of the sample was determined by measuring the absorbance; the HI-6 absorption band had a wavelength of 300 nm.

2.8 Animals. All experiments conformed to the guidelines of the Regulations of the Experimental Animal Administration issued by the State Committee of Science and Technology of the People's Republic of China (November 14, 1988). Zebrafish (4 weeks old) were provided by the School of Life Science of Peking University (Beijing, China) and were reared according to standard methods.³³ Kunming mice (4 weeks old) and Sprague-Dawley rats (10 weeks old; both specific pathogen-free) were purchased from the Animal Center of the Academy of Military Science. Rodents had free access to sterilized food and distilled water and were maintained in stainless steel cages filled with hardwood chips in an air-conditioned room on a 12:12-h light/dark cycle.

2.9 Confirmation of TF-MSN brain targeting in zebrafish by confocal laser scanning microscopy (CLSM). Zebrafish were randomly divided into control and experimental groups, and 10 nl of TF-MSN, MSN, and FITC-doped TPNP suspension were injected into the heart using a micro-sprinkler. After 10 min, the brain was

visualized and imaged by CLSM at 100 \times magnification and an excitation wavelength of 470 nm.

2.10 Confirmation of TF-MSN brain targeting in Kunming mice by transmission electron microscopy (TEM). Kunming mice were injected with a TF-MSN suspension (3 mg ml⁻¹, 200 μ l) through the tail vein. The brain was cut into small pieces (3 \times 3 mm) and fixed with glutaraldehyde (2%) and osmic acid (1%) in phosphate-buffered saline (PBS, pH 7.4) for 4 h at 4 $^{\circ}$ C, then dehydrated, embedded, and sectioned at a thickness of 4 μ m. Sections were stained with hematoxylin and eosin (H&E), uranium acetate, and lead citrate in the dark for 10 min each and visualized by TEM to detect MSNs.

2.11 Measurement of the reactivation rate (RR) in vivo. Kunming mice were randomly divided into four groups (n = 10 each): untreated non-poisoned controls (group 1), untreated soman-poisoned (140 μ g kg⁻¹ soman; group 2), soman-poisoned and treated with aqueous HI-6 solution (2.2 mg ml⁻¹ solution at a dose of 10 μ l g⁻¹; group 3), and soman-poisoned and treated with HI-6-loaded TF-MSN suspension (3.0 mg ml⁻¹ TF-MSN, 2.2 mg ml⁻¹ HI-6 at a dose of 10 μ l g⁻¹; group 4). The antidote was injected immediately after soman poisoning; 10 min later, blood and brain samples were collected from each group. Brain tissue was homogenized and centrifuged to obtain supernatants for analysis. Blood or tissue supernatant diluted 50-fold (20 μ l) was added to four wells of an EIA/RIA plate (Costar 9018; Sigma-Aldrich, St. Louis, MO,

USA). Adrenocorticotrophic hormone (30 μl of a 1% solution) and PBS (30 μl of a 0.1 M solution) were added to two wells each. After incubation for 30 min at 37°C, 5,5-dithiobis-2-nitrobenzoic acid (200 μl of a 1% solution) was added to each well and the optical density (OD) was measured at a wavelength of 415 nm. RR was calculated using the equation $\text{RR (\%)} = (\text{OD}_{415 \text{ nm}} [\text{group 3}] - \text{OD}_{415 \text{ nm}} [\text{group 2}]) / (\text{OD}_{415 \text{ nm}} [\text{group 1}] - \text{OD}_{415 \text{ nm}} [\text{group 2}])$.

2.12 Histopathological analysis of brain sections. Kunming mice were divided into the same four groups as for RR measurement. The brains were fixed in glutaraldehyde (3%) for 48 h. After dehydration and embedding, the tissue was cut into 4- μm sections and stained with H&E. Sections were visualized by light microscopy.

2.13 Measurement of therapeutic factor. Kunming mice were divided into groups 2, 3, and 4 as described above and injected with various doses of soman ranging from 120 to 260 $\mu\text{g kg}^{-1}$ ($n = 10$ mice at each concentration). The number of surviving mice was counted 24 h later. The median lethal dose (LD_{50}) was calculated using SPSS software (SPSS Inc., Chicago, IL, USA). The therapeutic factor for each condition was calculated using the equation $\text{therapeutic factor} = \text{LD}_{50} \text{ antidote} / \text{LD}_{50} [\text{group 2}]$.

2.14 Measurement of acute/sub-acute toxicity of the DS. Sprague-Dawley rats were intravenously injected with DS suspension at a dose of 4.2–8.2 mg/rat three times a week for 2 weeks (for a total of six injections). The weight of each rat was recorded

daily, as was overall health including presence of infection or ascites and changes in mobility and food consumption. Rats were sacrificed on day 14. The blood and major organs (heart, liver, spleen, lungs, kidneys, muscle, stomach, intestines, great omentum, testicles, and ovaries) were collected. The complete blood count and biochemical parameters in serum were measured, and the liver, spleen, kidneys, brain, heart, testicles, and ovaries were weighed to obtain a coefficient for each group. All tissues were processed in the same manner as the brain and were examined histologically for abnormalities or lesions.

2.15 Measurement of MSN excretion from the brain. Kunming mice were injected with TF-MSN suspension (3 mg ml^{-1}) intravenously and the brains were collected at predetermined time points, washed with saline to remove residual blood, and weighed. After digesting in H_2O /hydrogen fluoride/ HNO_3 (1:1:1) with heating, Si content of the mixture was analyzed by inductively coupled plasma mass spectroscopy (ICP-MS). The Si level of the samples of feeding grain and blank mice brains (without any treatment/injected) were measured as described before.

2.16 Morris water maze test. Kunming mice were randomly divided into two untreated and TF-MSN treatment groups ($n = 10$ mice each). The treatment group was intravenously injected with TF-MSN suspension (3.0 mg ml^{-1} , $10 \text{ } \mu\text{l g}^{-1}$) three times a week for 2 weeks (for a total of six injections). The Morris water maze consisted of a black circular pool (diameter \times height, $100 \times 50 \text{ cm}$) divided into four quadrants. A

platform with a diameter of 9 cm was placed 1 cm below the surface of the water in the middle of the target quadrant. Mice were trained to find the platform over 4 days after being placed in each quadrant. The time spent to locate the platform was recorded for each trial. After removal of the platform, the number of platform crossings, escape latency, and time spent in the target quadrant were recorded using a tracking system on day 5 of the test.

3 Result and discussion

Design and synthesis of the DS and TPNPs. The DS consisted of an MSN core with a transferrin (TF)^{34, 35} shell. The TF receptor is highly expressed on the BBB surface³⁶ and it was therefore predicted that TF-MSNs would cross the BBB by a receptor-mediated transport mechanism. HI-6, which cannot enter the brain on its own, was loaded onto TF-MSNs (Fig. 1A) and was rapidly released via direct channels from the particle matrix into the environment to antagonize soman and thereby restore ACh degradation (Fig. 1B). TPNPs³⁵ loaded with HI-6 were synthesized for comparison. HI-6 was assembled into a nanocore coating via a shell of polymer PLGA and was released from the TPNPs at a low speed as a result of PLGA degradation.

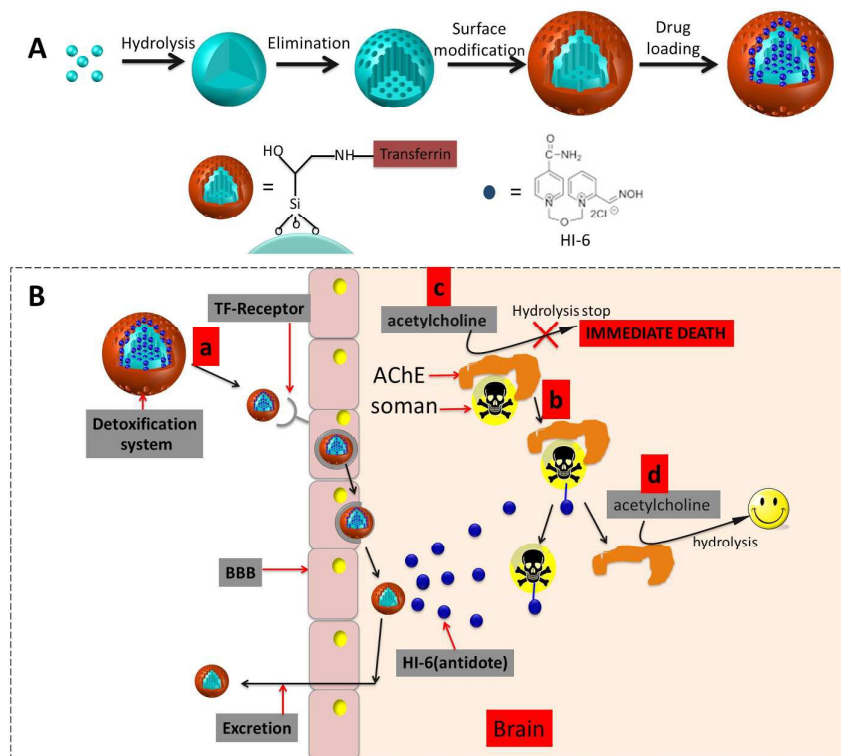


Figure 1. Schematic illustration of (A) the preparation of TF-MSNs loaded with HI-6; and (B) the detoxification process: TF-MSNs approach and cross the BBB, the drug is released, and TF-MSNs are excreted (a); reactivated AChE induces acetylcholine hydrolysis (b), which was inhibited by soman and would result in death (c), allowing normal ACh hydrolysis to resume (d).

By precisely adjusting the pH of the solution, MSNs with a roughly spherical shape and diameter of 100 nm^{22, 37} were prepared via silane hydrolysis (Fig. 2). FITC was mixed with the particles to allow imaging and spectroscopic measurements. The mesoporous structure was formed by eliminating surfactant from the particles (Fig. 2A, B). The MSN surface was then coated with a TF layer at a thickness of almost 5–10 nm using an organo-silane linker (Fig. 2C, Tab 1 dynamic light scattering (DLS)), and HI-6 added to the system entered the MSN pores. The DS was re-suspended in saline and stored at -20°C to preserve TF activity.

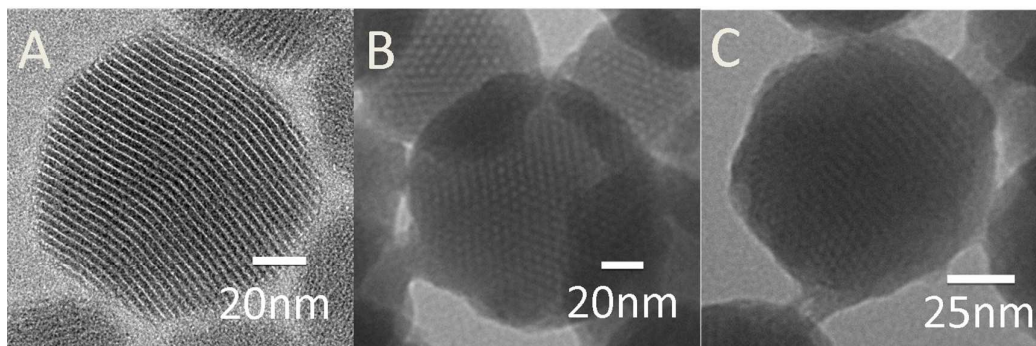


Figure 2. (A–C) Transmission electron micrographs of unmodified MSNs from different views (A, B), and of MSNs modified with a TF coating.

The details of MSN and DS were further characterized by a series of measurements. After eliminating the pore forming agent (CTAB), the surface area of the NPs was increased five times owing to the mesoporous structure formed, as revealed by the BET method. The observed protein layer thickness (5 nm) and MSN pore size (4.96 nm) were consistent with the data obtained from TEM. In contrast, the diameter of NPs as determined by the DLS method was little larger than that from TEM, which might be explained by the different calculation techniques between the two methods. After TF coating, approximately 115 TF molecules were linked on the surface of each MSN as determined from the TF concentration assayed using a BCA protein assay kit and the density of MSN from the BET method. The surface charge of the NPs changed from positive to negative in PBS after TF coating. Furthermore, despite tiny differences in different solvent media, all of the NPs were stable and well dispersed.

Table 1: Hydrodynamic size, surface charge (DLS section), and Nitrogen sorption data (BET section) of silica nanoparticles in different preparation stages

		SNP	MSN	TF-MSN	
DLS	size (nm)	PBS	/	169.6	182.8
		CCM	/	168.9	178.5
		SCM	/	258.1	265.9
	Zeta potential (mv)	PBS	/	48.1	-18.7
		CCM	/	-16.2	-9.23
		SCM	/	-10.9	-9.92
BET	Surface area (m/g)	208.1	1025.6	576.3	
	Pore size (nm)	12.46	4.96	6.17	

DLS:dynamic light scattering

BET:Brunner-Emmett-Teller method

PBS:phosphate buffered saline

CCM:cell culture media

SCM:serum containing media

SNP:solid nanoparticles

TF-MSN: transferrin modified MSN

MSN: mesoporous silica nanoparticles

“/” : untested

The complete DS preparation process was revealed and monitored by evaluating the appearance or disappearance of specific peaks in the UV-visible absorption spectrum (Fig. 3A) and high-angle X-ray powder diffraction (XRD) (Fig. 3B). Before surface modification with TF, MSNs doped with FITC exhibited a strong characteristic absorption peak at 500 nm but no peak was observed in the XRD pattern. After adding the protein coating, this UV absorption peak of MSN was diminished, consistent with previous reports,³⁸ and the XRD pattern of TF-MSN displayed sharp peaks around $2\theta = 27^\circ$, 32° , 45° , and 66° , which might have been derived from the protein. The loading of HI-6 was confirmed by the appearance of the characteristic UV absorption peak of HI-6 at 300 nm and the XRD peaks around $2\theta = 17^\circ$ and 25° .

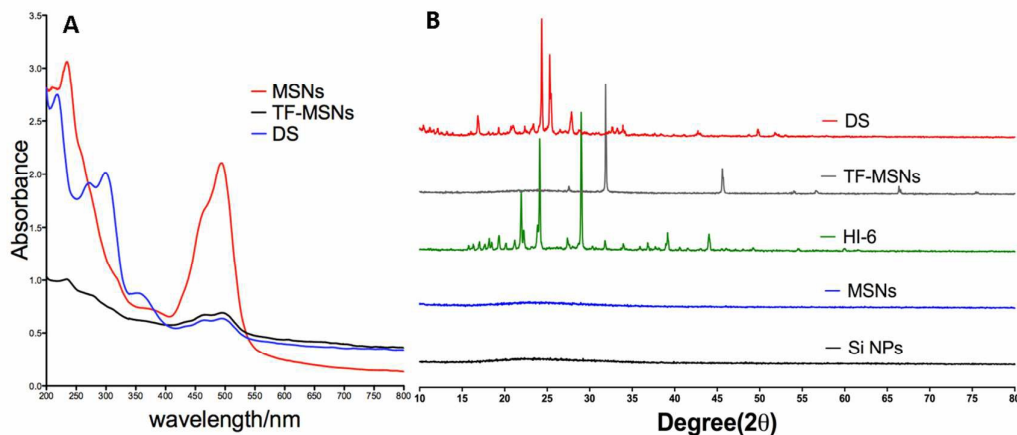


Figure 3. (A) UV-visible spectra of MSNs, TF-MSNs, and TF-MSNs loaded with HI-6 (DS) (B) high angle powder X-ray diffraction patterns of DS, TF-MSNs, HI-6, MSNs), and Si NPs.

Drug loading and release behavior. Both MSN and TF-MSN loaded drugs via capillary absorption within the mesoporous structure. The drug loading ratio was increased with the increasing input dosage of HI-6 (Fig. 4A red and blue lines). However, the drug encapsulation ratio remained constant (Fig. 4A black and green lines), which meant that the drug input dosage had no influence on the encapsulation ability and that the encapsulation ratio of the NPs might be regulated by inherent factors such as surface area.²⁷ Furthermore, both of the TF-MSN encapsulation ratios were higher than those of MSN, which might be due to the extra absorption by the outside protein layer.³⁹

For the DS to be an effective antidote for soman, it must rapidly release the loaded AChE-reactivating drug. TF-MSNs released 40% of loaded HI-6 within 30 min, as determined by a dialysis experiment (Fig. 4B). However, the DS showed slower HI-6 release compared to free HI-6 solution owing to capillary action of the pores, which ensured that sufficient amounts of HI-6 were present when the DS was

transported into the brain²⁰ as the majority of the loaded drug was not lost during transport across the BBB. In contrast, only 10% of HI-6 was released from TPNP during the period of measurement, which is inadequate for effective brain detoxification. These results demonstrate that the release behavior of the MSNs is suitable for acute detoxification.

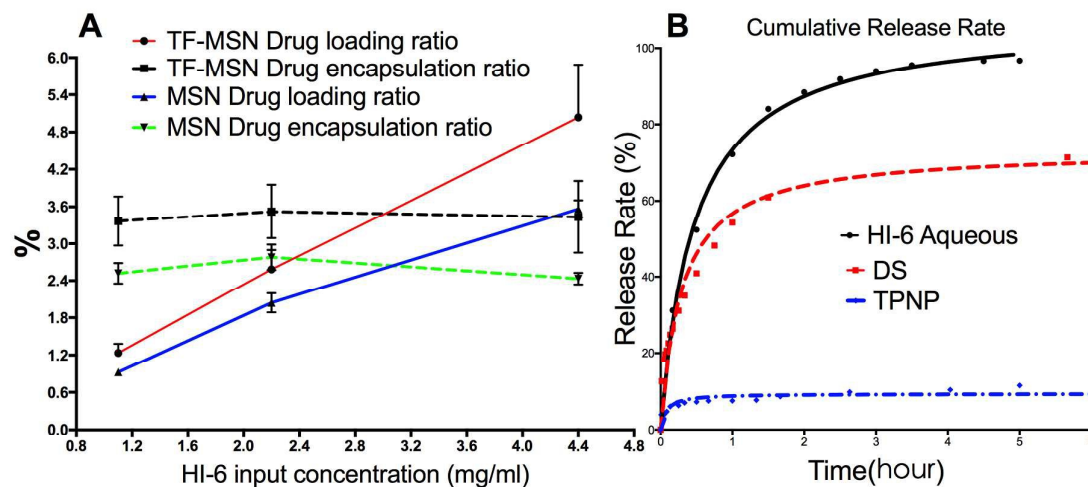


Figure 4. (A) Drug loading and encapsulation ratio profiles of MSN and TF-MSN. (B) Release profiles of HI-6 from aqueous solution, HI-6-loaded TF-MSNs (DS), and TPNP.

Brain-targeting effect. We examined the brain-targeting effect of TF-MSNs in vivo using zebrafish, a small teleost fish with a transparent body and a BBB with a structure similar to that of mammals.⁴⁰ CLSM was used to visualize FITC fluorescence in live animals. A strong fluorescence signal was observed in the zebrafish brain⁴⁰ after TF-MSNs were injected into the heart (Fig. 5C). In contrast, zebrafish injected with TPNPs plus FITC also showed a substantial fluorescence signal in the brain (Fig. 5D), whereas injection of MSNs without TF modification showed little fluorescence (Fig. 5B). The experiment was also performed in Kunming mice, wherein TF-MSNs injected

intravenously were clearly observed in hippocampal neurons by TEM (Fig. 5E, F), demonstrating that TF targets the MSNs to the brain for BBB penetration.

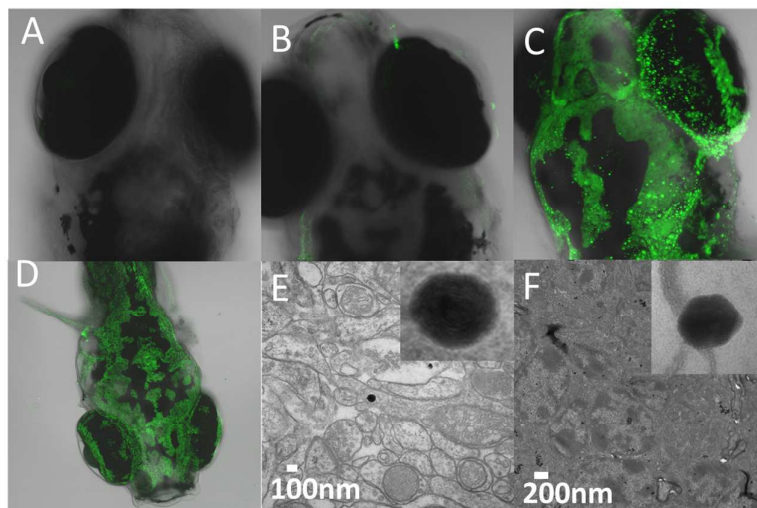


Figure 5. Confocal laser scanning micrographs of brain sections from (A) normal zebrafish and zebrafish treated with (B) unmodified MSNs, (C) TF-MSNs, and (D) fluorescent TPNPs. (E, F) Transmission electron micrographs of the cortex of a Kunming mouse; high-magnification views of MSNs are shown in the insets.

Pharmacodynamics analysis. The RR was measured in vivo according to a standard method of assessing the efficacy of NA antidotes.⁴¹ Following soman poisoning, the DS and HI-6 aqueous solution containing the same concentration of HI-6 were injected into mice via the tail vein, and AChE activity in the blood and brain was tested. The RR of the DS and aqueous HI-6 solution in blood were both > 20% (Fig. 6A), implying that HI-6 released from the DS into the peripheral circulation would have the same capacity for reactivation as the HI-6 in aqueous solution. However, in the brain the RR was > 20% only in the group treated with DS (Fig. 6B), which is the highest value reported to date and nearly six times higher than that of HI-6 solution (3%). This suggests that HI-6 was efficiently transported across the BBB and rapidly released in the brain. Without

TF-MSNs as nanocarriers, the HI-6 solution was only effective in the peripheral circulation. In contrast, the RR of the TPNP-treated group was < 10% in both the blood and brain, confirming that there was little HI-6 released owing to the polymer-coated nanostructure and indicating that the speed of drug release has a significant and direct effect on detoxification.

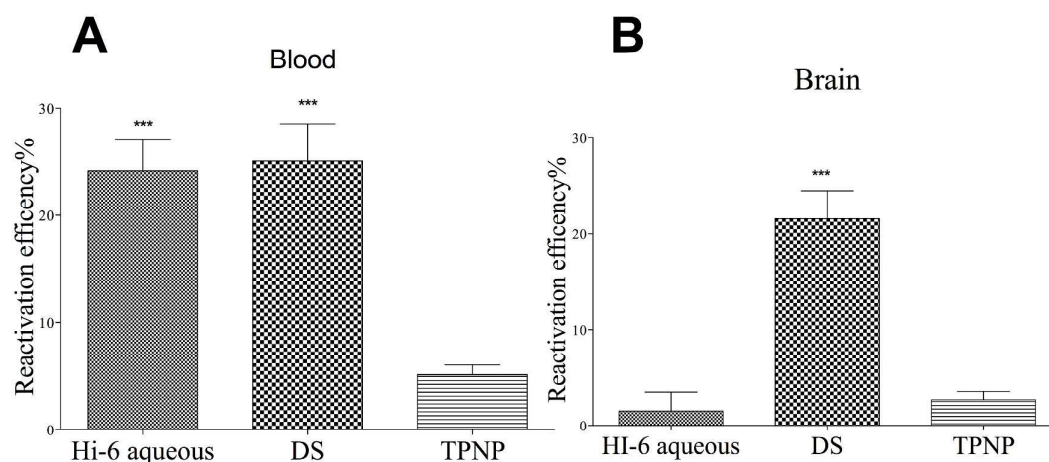


Figure 6. (A, B) RR of HI-6 aqueous solution, HI-6-loaded TF-MSNs (DS), and HI-6-loaded TPNPs in the blood (A) and brain (B). *** $P < 0.001$ vs. TPNP group (A) and vs. HI-6 aqueous group (B) ($n = 8$ per group).

The high level of RR in the group injected with DS indicated superior protective effects in brain tissues and high therapeutic efficacy. Morphological assessment of brain sections revealed the formation of large edemas and cell apoptosis in the cerebral cortex and hippocampal CA2 region of soman-poisoned mice that were either untreated (Fig. 7A, E) or treated with aqueous HI-6 solution (Fig. 7B, F). In the DS-treated group, there was some apoptosis detected in both brain regions (Fig. 7C, G); however, the hippocampal pyramidal cells had normal morphology (Fig. 7D, H). The therapeutic

factor is an index of the curative effect. For the DS, the value was 1.73 (Table 2), which is about 57% higher than that of the currently used drug K203 and is the highest value reported to date.⁴² These results indicate that reversing soman-mediated inhibition of AChE in the brain alleviates the symptoms of toxicity arising from a hyperactivated cholinergic system and increases survival rates in cases of soman poisoning.⁴³

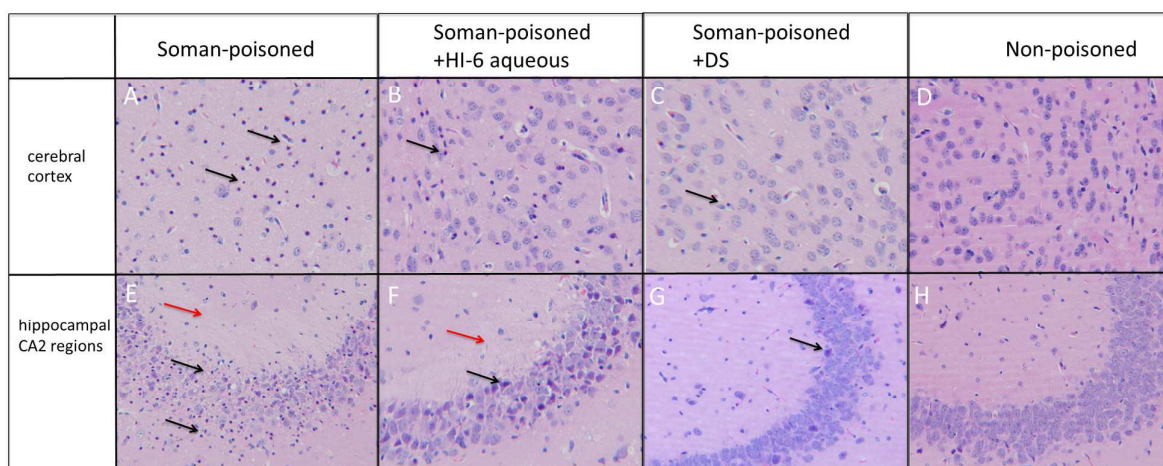


Figure 7. Histopathology of the cerebral cortex (A–D) and hippocampal CA2 region (E–H) of mice poisoned with soman (A, E) and treated with aqueous HI-6 (B, F) or HI-6-loaded TF-MSN (DS) (C, G); and in non-poisoned mice (D, H). Black arrows indicate pyknotic cells with strong cytoplasmic staining and nuclear condensation. Red arrows indicate edema. Images are shown at 200 \times magnification.

Table 2. Therapeutic effects of intramuscularly administered agents in soman-poisoned mice

Treatment	Dose ^a (mg·kg ⁻¹)	LD ₅₀ ^b (μg·kg ⁻¹)	Therapeutic ratio ^c
-----------	--	--	--------------------------------

Untreated	-	148	-
Aqueous HI-6	22	200.4	1.37
DS ^d	22	264.55	1.73
K203	15		1.1
MMB-4 ^e	15		1.07

^aDrugs were injected in volumes of 0.05 ml·g⁻¹ of body weight.

^bLethal dose (LD₅₀) of soman.

^cTherapeutic factor = LD₅₀ of soman in treated animals/LD₅₀ in untreated animals.

^dHI-6-loaded TF-MSN.

Safety and biocompatibility of the DS. To date, the safety of MSNs in the brain has not been adequately demonstrated.^{22, 28, 44} Following detoxification with TF-MSNs, the amount of residual Si in the brain and the background Si levels (both the dietary sources and the native Si content in mice without treatments) were accurately quantified by ICP-MS. The concentration of Si in the brain was maximal 10 min after injection and decreased thereafter for up to 7 days, by which time the level had decreased by nearly 92.4% (Fig. 8). Although the precise mechanism of Si excretion remains unknown, the process is likely facilitated by efflux proteins of the BBB. Residual MSN in the brain is excreted from the body in the form of urine and stools, as previously demonstrated.⁴⁵ Furthermore, there is very little inherent Si contained in the native mouse brains (0.6788 μg g⁻¹) which might due to the natural ingredient diets of high Si content (1719.5 μg g⁻¹). But the Si content in brains in the treated mice is nearly 4 times than the native untreated ones, which indicate that the influence of diets could be ignored. And all of the mice are fed with the same natural ingredient diets, so the trend that the

level of Si decreases in brain was not influenced by the background of diets. Overall, it is important that minimal MSNs accumulate in the body or especially in the brain after DS intravenous administration.

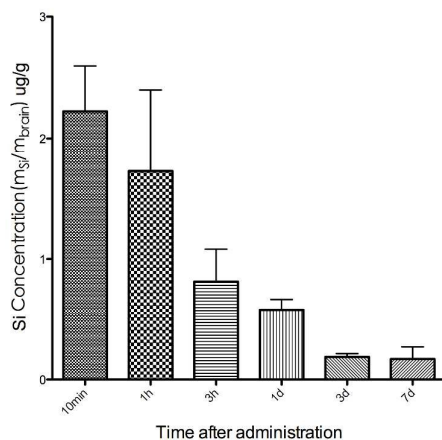


Figure 8. Si concentration in the brain following TF-MSN treatment. Mice (n = 2 per group) were injected with TF-MSNs (3 mg ml^{-1}) through the tail vein and the Si levels were measured by ICP-MS at the indicated time points (up to 7 days after injection).

Despite the non-biodegradability of residual MSN in the brain, no lesions or histopathological abnormalities were noted (Fig. 7D, H). Mice were subjected to behavioral evaluation with the Morris water maze test. No differences were noted between mice treated with TF-MSN and untreated mice in terms of time spent in the target quadrant, number of platform crossings, and latency to first entry (Fig. 9). These results indicate that residual TF-MSNs in the brain had no effect on spatial learning and memory and that TF-MSNs are safe for use as a brain-targeted DS.

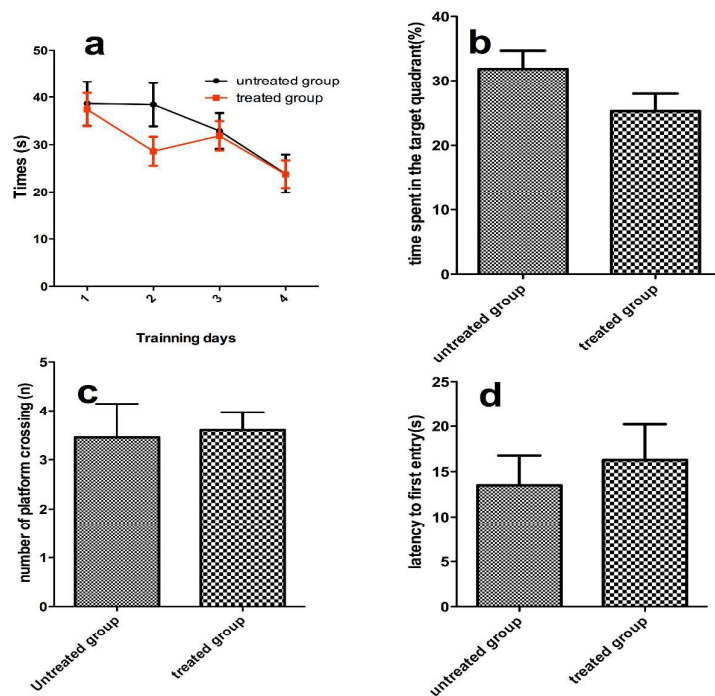


Figure 9. Effect of TF-MSNs on the cognitive performance of mice in the Morris water maze. Mice were treated with TF-MSN (3.0 mg ml^{-1} or $10 \mu\text{l g}^{-1}$) for 14 days. (A) Escape latency during the 4 training days. (B) Percentage of time spent in the target quadrant on day 5. (C) Number of platform crossings on day 5. (D) Escape latency.

Given the intended application of TF-MSNs in emergency situations, their acute toxicity was evaluated to determine the potential for secondary injury. Rats were injected through the tail vein three times a week for 14 day at various therapeutic doses and their condition monitored for 1 month. During this period, there were no changes in weight (Fig. S1), mobility, or feeding behavior and no infection or ascites in TF-MSN-treated relative to untreated rats. In addition, there was no inflammation induced by TF-MSN treatment, as determined by blood tests (Table S1), the histological analysis of primary organs (Fig. 10),²² and organ coefficients (Table S2).

However, the level of creatine kinase, a marker of cardiovascular damage, was above the normal range, and mild epithelial cell swelling and lymphocytic infiltration was observed in the kidneys of animals treated with a high dose of TF-MSN (i.e., twice the working concentration). Therefore, although TF-MSNs were considered safe for emergency detoxification, they should be used at an appropriate concentration to prevent tissue damage.

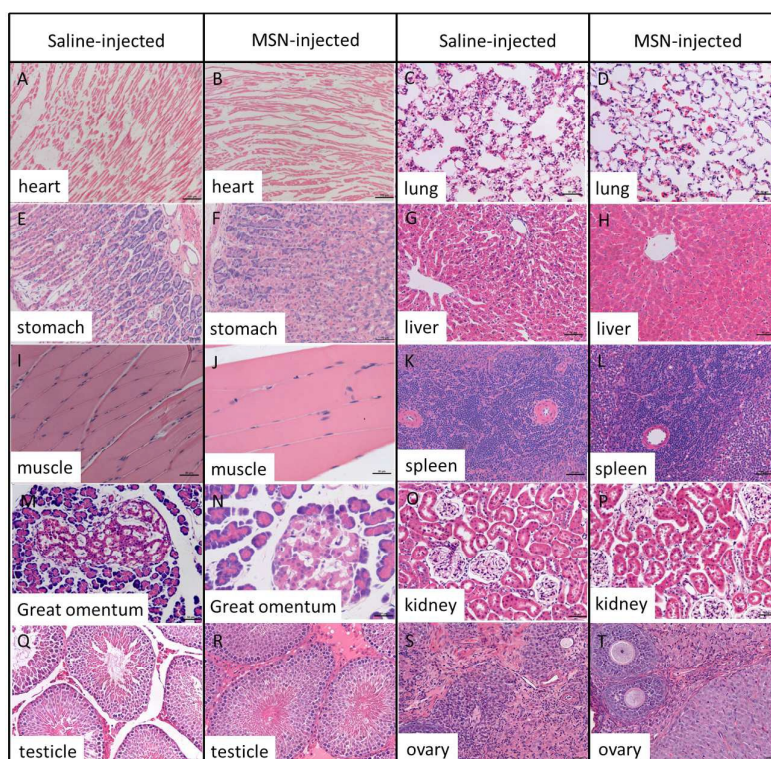


Figure 10. Histopathology of the primary organs of mice injected with saline or TF-MSNs. Other than the kidneys of TF-MSN-treated mice, which showed mild epithelial cell swelling and lymphocytic infiltration, there were no pathological changes observed in any organs in either group.

4 Conclusion

HI-6-loaded TF-MSNs are the most effective antidote against soman reported to date owing to their rapid release of the loaded drug and their ability to penetrate the BBB. When delivered by TF-MSNs to the brain, HI-6 effectively reactivated soman-inhibited cerebral AChE, conferring a neuroprotective effect and decreasing mortality rates in soman-poisoned mice. The MSNs were determined to be safe for use based on the observation that nearly 92.4% was excreted from the brain 1 week after administration, with the residual MSNs causing no obvious side effects. These findings represent the successful repurposing of a well-known nanomaterial to obtain an urgently required therapeutic effect that cannot be achieved with existing drugs.

Supporting Information. This material is available free of charge on the internet at <http://www.rsc.org>

Acknowledgments

This work was supported by the National Natural Science Foundation of China (No 81402847), the Youth Foundation of General Logistics Department of PLA (No 13QNP152), and a Military Medical Scientific and Technological Project for the “Twelfth Five-year Plan” (AWS11C004, BWS12J042).

References

1. A. Verweij, H. L. Boter and C. E. A. M. Degenhardt, *Science*, 1979, **204**, 616-618.
2. K. Kim, O. G. Tsay, D. A. Atwood and D. G. Churchill, *Chemical reviews*, 2011, **111**, 5345-5403.

3. T. Okumura, T. Hisaoka, T. Naito, H. Isonuma, S. Okumura, K. Miura, H. Maekawa, S. Ishimatsu, N. Takasu and K. Suzuki, *Environmental toxicology and pharmacology*, 2005, **19**, 447-450.
4. E. Dolgin, *Nature medicine*, 2013, **19**, 1194-1195.
5. D. M. Quinn, *Chemical Reviews*, 1987, **87**, 955-979.
6. S. Ehrenpreis, 1964.
7. G. C. R. Jr and C. T. Condurache, *Clinical Pharmacology & Therapeutics*, 2010, **88**, 319.
8. G. Mercey, T. Verdelet, G. Saint-André, E. Gillon, A. Wagner, R. Baati, L. Jean, F. Nachon and P.-Y. Renard, *Chemical Communications*, 2011, **47**, 5295-5297.
9. P. Ballabh, A. Braun and M. Nedergaard, *Neurobiology of disease*, 2004, **16**, 1-13.
10. G. Miller, *Science*, 2002, **297**, 1116-1118.
11. J. Kassa, J. Ž. á. Karasová and M. Krejčiová, *Journal of Applied Biomedicine*, 2013, **11**, 7-13.
12. M. Dadparvar, S. Wagner, S. Wien, J. Kufleitner, F. Worek, H. von Briesen and J. Kreuter, *Toxicology letters*, 2011, **206**, 60-66.
13. F. M. Kievit and M. Zhang, *Advanced Materials*, 2011, **23**, H217-H247.
14. H. Ding, S. Inoue, A. V. Ljubimov, R. Patil, J. Portilla-Arias, J. Hu, B. Konda, K. A. Wawrowsky, M. Fujita and N. Karabalin, *Proceedings of the National Academy of Sciences*, 2010, **107**, 18143-18148.
15. D. Brambilla, B. Le Droumaguet, J. Nicolas, S. H. Hashemi, L.-P. Wu, S. M. Moghimi, P. Couvreur and K. Andrieux, *Nanomedicine: Nanotechnology, Biology and Medicine*, 2011, **7**, 521-540.
16. H. Gao, Z. Pang and X. Jiang, *Pharmaceutical research*, 2013, **30**, 2485-2498.
17. H. Guerrero-Cázares, S. Y. Tzeng, N. P. Young, A. O. Abutaleb, A. Quiñones-Hinojosa and J. J. Green, *Acs Nano*, 2014, **8**, 5141-5153.
18. R. M. Koffie, C. T. Farrar, L.-J. Saidi, C. M. William, B. T. Hyman and T. L. Spires-Jones, *Proceedings of the National Academy of Sciences*, 2011, **108**, 18837-18842.
19. G. A. Hughes, *Nanomedicine: nanotechnology, biology and medicine*, 2005, **1**, 22-30.
20. J. Kufleitner, S. Wagner, F. Worek, H. von Briesen and J. Kreuter, *Journal of microencapsulation*, 2010, **27**, 506-513.
21. I. Izquierdo-Barba, E. Sousa, J. C. Doadrio, A. L. Doadrio, J. P. Pariente, A. Martínez, F. Babonneau and M. Vallet-Regí, *Journal of sol-gel science and technology*, 2009, **50**, 421-429.
22. J. Lu, M. Liong, Z. Li, J. I. Zink and F. Tamanoi, *Small*, 2010, **6**, 1794-1805.
23. V. Mamaeva, C. Sahlgren and M. Lindén, *Advanced drug delivery reviews*, 2013, **65**, 689-702.
24. Q. He and J. Shi, *Adv Mater*, 2014, **26**, 391-411.
25. E. D. Davis, W. O. Gordon, A. R. Wilmsmeyer, D. Troya and J. R. Morris, *The Journal of Physical Chemistry Letters*, 2014, **5**, 1393-1399.

26. P. Xu, S. Guo, H. Yu and X. Li, *Small*, 2014, **10**, 2404-2412.
27. P. Xu, H. Yu, S. Guo and X. Li, *Analytical Chemistry*, 2014, **86**, 4178-4187.
28. D. J. Bharali, I. Klejbor, E. K. Stachowiak, P. Dutta, I. Roy, N. Kaur, E. J. Bergey, P. N. Prasad and M. K. Stachowiak, *Proceedings of the National Academy of Sciences of the United States of America*, 2005, **102**, 11539-11544.
29. J. G. Clement, *Biochemical pharmacology*, 1982, **31**, 1283-1287.
30. H. P. M. van Helden, H. J. van der Wiel, J. de Lange, R. W. Busker, B. P. C. Melchers and O. L. Wolthuis, *Toxicology and applied pharmacology*, 1992, **115**, 50-56.
31. S. Wagner, J. Kufleitner, A. Zensi, M. Dadparvar, S. Wien, J. Bungert, T. Vogel, F. Worek, J. Kreuter and B. H. Von, *Plos One*, 2010, **5**, : e14213.
32. E. A. Carlos, D. Debra, W. Meocha, K. Lavrent and M. S. Cristina, *Acs Nano*, 2011, **5**, 9313-9325.
33. M. Westerfield, *W47 1993*, 1993.
34. K. Ulbrich, T. Hekmatara, E. Herbert and J. Kreuter, *European Journal of Pharmaceutics and Biopharmaceutics*, 2009, **71**, 251-256.
35. J. Chang, Y. Jallouli, M. Kroubi, X.-b. Yuan, W. Feng, C.-s. Kang, P.-y. Pu and D. Betbeder, *International journal of pharmaceutics*, 2009, **379**, 285-292.
36. L. Descamps, M.-P. Dehouck, G. Torpier and R. Cecchelli, in *Biology and Physiology of the Blood-Brain Barrier*, Springer, 1996, pp. 51-54.
37. E. Tasciotti, X. Liu, R. Bhavane, K. Plant, A. D. Leonard, B. K. Price, M. M.-C. Cheng, P. Decuzzi, J. M. Tour and F. Robertson, *Nature nanotechnology*, 2008, **3**, 151-157.
38. D. Liu, R. C. Huxford and W. Lin, *Angewandte Chemie*, 2011, **123**, 3780-3784.
39. B. Li, F. Nachon, M.-T. Froment, L. Verdier, J.-C. Debouzy, B. Brasme, E. Gillon, L. M. Schopfer, O. Lockridge and P. Masson, *Chemical research in toxicology*, 2007, **21**, 421-431.
40. J.-Y. Jeong, H.-B. Kwon, J.-C. Ahn, D. Kang, S.-H. Kwon, J. Park and K.-W. Kim, *Brain research bulletin*, 2008, **75**, 619-628.
41. F. Worek, P. Eyer and H. Thiermann, *Drug testing and analysis*, 2012, **4**, 282-291.
42. M. Čalić, A. L. Vrdoljak, B. Radić, D. Jelić, D. Jun, K. Kuča and Z. Kovarik, *Toxicology*, 2006, **219**, 85-96.
43. J. Bajgar, J. Fusek, J. Kassa, D. Jun, K. Kuca and P. Hajek, *Chemico-biological interactions*, 2008, **175**, 281-285.
44. R. Kumar, I. Roy, T. Y. Ohulchanskyy, L. A. Vathy, E. J. Bergey, M. Sajjad and P. N. Prasad, *ACS nano*, 2010, **4**, 699-708.
45. F. Barandeh, P.-L. Nguyen, R. Kumar, G. J. Iacobucci, M. L. Kuznicki, A. Kosterman, E. J. Bergey, P. N. Prasad and S. Gunawardena, *PloS one*, 2012, **7**, e29424.